provided with the imaging system and a simple procedure. After the region of interest was set in the kidney parenchyma, a movie was played back, and arrival times were sequentially calculated for each liver parenchyma pixel, and the time point at which 80% of the region of interest was enhanced by the contrast medium was defined as time 0. Next, a color map was automatically superimposed on a B-mode image. Although the display color could be freely adjusted, pixel colors were determined according to the following criteria. In a pilot study conducted on chronic hepatitis C, there was an interval of about 10 seconds between kidney enhancement and completion of liver enhancement. Therefore, 5 seconds, half of the arrival time determined in the pilot study, was used as the cutoff point. Pixels with an arrival time of 0 to 5 seconds were displayed in red, and those with an arrival time of 5 to 10 seconds were displayed in yellow (Figures 1 and 2). In this pilot study, Sonazoid-enhanced sonography was performed on 12 patients with liver disease in chronic hepatitis C infection. After infusion of Sonazoid, using a stopwatch preset at 0, we timed the period between the time the contrast agent reached the kidney and the time the contrasting of the entire liver was completed. The study was performed by 2 physicians. The results from the first and second physicians showed that the mean times needed for the enhancement were 9.6 and 10.4 seconds, respectively, and we used the average, namely 10 seconds, in this study.

Measurement of the Red Area

For quantitative evaluation of the obtained arrival time parametric imaging data, the ratio of the area of red pixels with shorter arrival times to the entire contrast-enhanced area was calculated as the "ratio of red" using ImageJ version 1.42 image analysis software (Wayne Rasband; National Institutes of Health, Bethesda, MD; Figure 3). It takes approximately 10 seconds for the contrast agent to reach the entire area of the liver. In this study, we used the median value (5 seconds) as a threshold. The regions where arrival of the contrast agent was detected within 5 seconds were depicted in red to calculate the ratio of red. A higher ratio means that the contrast agent arrival time in the liver is closer to that in the kidney; in other words, a wider area of the liver parenchyma received the contrast agent through the arterial route, indicating a shift in the arterial-portal blood flow balance toward arterial domination in the liver. Two anonymous physicians calculated the ratio of red. Both were physicians trained in the use and interpretation of contrast agents in the liver. They were not involved in sonographic scanning and were blinded to the identification, clinical history, and other imaging findings of the patients. The ratio of red was analyzed jointly by the physicians. Using the ImageJ software, one of them measured the ratio, and the other examined each case while evaluating the accuracy of the ratio measurement performed by the former physician. The results of the ratio of red analysis are presented in Table 1.

Figure 1. Contrast enhancement pattern of the liver parenchyma 10 seconds after arrival of the contrast medium following bolus infusion of Sonazoid via the median cubital vein: Sonazoid-enhanced images of the liver parenchyma with (right) and without (left) arrival time parametric imaging.

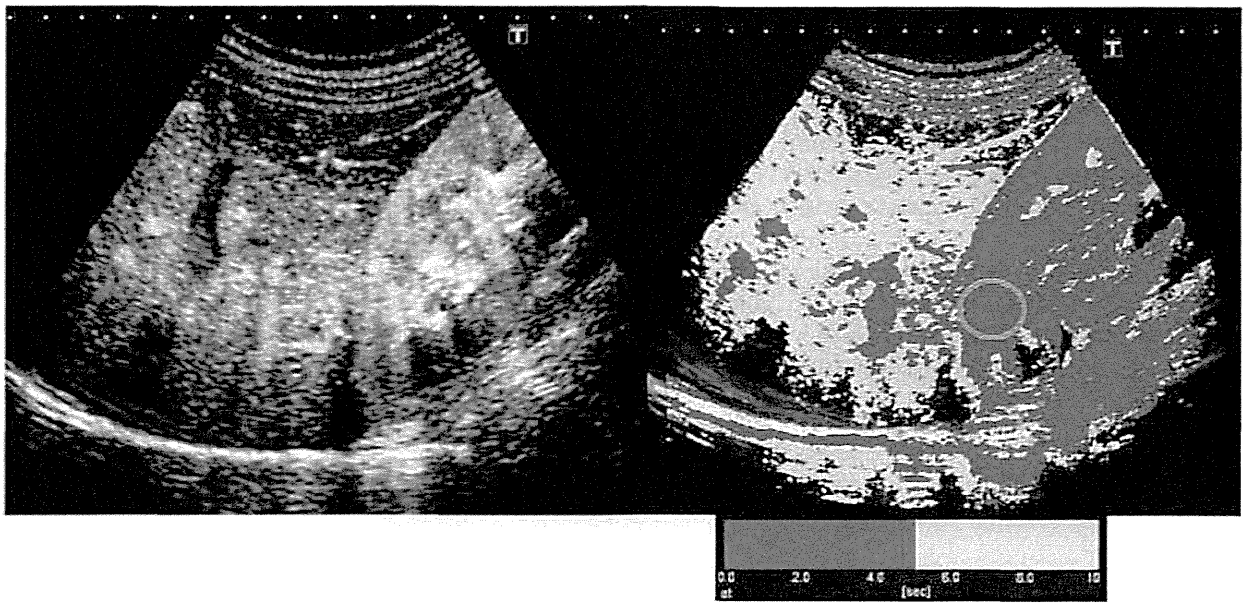

Ability of the Ratio of Red to Evaluate the Degree of Progression of Chronic Liver Disease

For each subject, the ratio of red was compared with fibrosis stage (F0–F4), serum albumin level, platelet count, and prothrombin time to determine its ability to evaluate the degree of progression of a chronic liver disease. Liver needle biopsies were performed after sonography with a 16-gauge liver biopsy needle (Core IITM semiautomatic biopsy instrument; InterV Clinical Products, Dartmouth, MA). The liver biopsy specimen was fixed in 10% formalin, paraffin embedded, sectioned, and stained with hematoxylin-eosin and azan for histologic evaluation. All liver biopsy specimens were evaluated by a single experienced pathologist (M.I.), who was unaware of the clinical conditions of the patients. Pathologic liver fibrosis was evaluated according to the Metavir scoring system.[6] Fibrosis was staged as follows: F0, no fibrosis; F1, portal fibrosis without septa; F2, portal fibrosis and few septa; F3, numerous septa without cirrhosis; and F4, cirrhosis (Figure 4).

Statistical Analysis

The Jonckheere-Terpstra trend test and Steel-Dwass test were used for the comparison of the ratio of red between fibrosis stages. Receiver operating characteristic (ROC) curves were used to determine the optimal cutoff value for fibrosis staging based on arrival time parametric imaging data. The area under the ROC curve was also determined. Moreover, we calculated positive and negative predictive values. Spearman rank correlation coefficients were used to examine the correlation of the ratio of red with the serum albumin level, platelet count, and prothrombin time as determined by blood examination. All analyses were performed using Excel Statistics 2008 statistical analysis soft-

Figure 2. Procedure for arrival time parametric imaging. After the region of interest is set in the kidney parenchyma, a movie is played back; arrival times are sequentially calculated for each liver parenchymal pixel; and the time point at which 80% of the region of interest is enhanced by the contrast medium is defined as time 0. Next, a color map is automatically superimposed on a B-mode image. Pixels with an arrival time of 0 to 5 seconds are displayed in red, and those with an arrival time of 5 to 10 seconds are displayed in yellow.

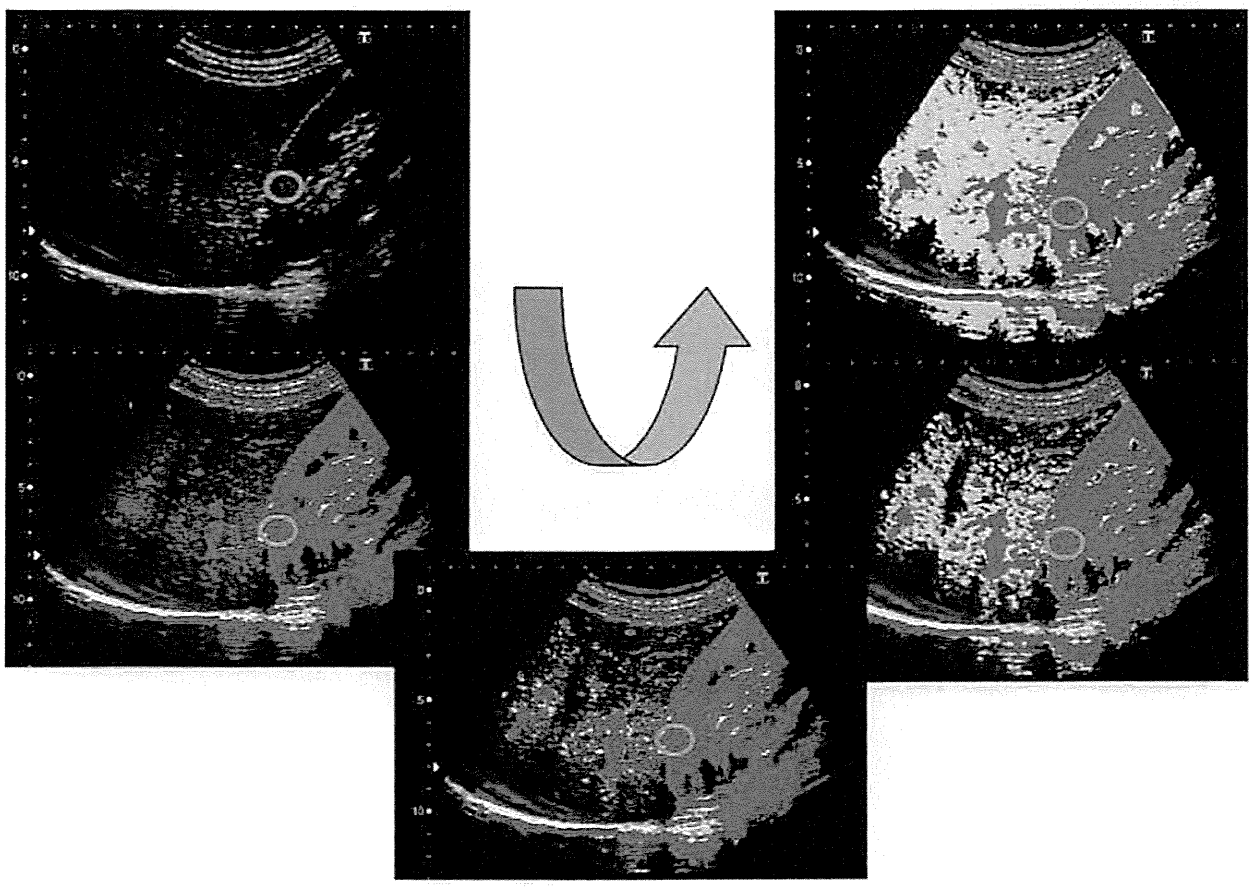

ware (SSRI Co, Tokyo, Japan). Differences were considered significant at $P < .05$.

Results

The clinical and biochemical characteristics of the healthy volunteers (n = 10) and patients with liver disease in chronic hepatitis C infection (n = 60) enrolled in this study are summarized in Table 2. The distribution of fibrosis stages as determined by liver biopsy in the 60 patients with liver disease was as follows: F1 in 25 patients, F2 in 20, F3 in 6, and F4 in 9. The ratio of red was calculated as 13.7% ± 5.7% for healthy controls, 18.7% ± 11.6% for F1 patients, 38.6% ± 22.2% for F2, 63.3% ± 16.7% for F3, and 84.3% ± 12.4% for F4 (Table 1). The Jonckheere-Terpstra test for the ratio of red variation trend in healthy controls and F1–F4 patients yielded $P < .0001$, showing a significant increasing trend in the ratio of red with the increasing stage of fibrosis. A multiple intergroup comparison using the Steel-Dwass test revealed significant differences between healthy controls and F2 patients ($P < .01$), healthy controls and F3 patients ($P < .05$), healthy controls and F4 patients ($P < .01$), F1 and F2 patients ($P < .01$), F1 and F3 patients ($P < .01$), F1 and F4 patients ($P < .01$), and F2 and F4 patients ($P < .01$; Figure 5), showing a significant increase in the ratio of red with the increasing stage of fibrosis.

The ratio of red was significantly negatively correlated with the serum albumin level ($r = -0.29$; $P = .027$), platelet count ($r = -0.46$; $P = .0003$), and prothrombin time ($r = -0.46$; $P = .0002$). Despite the weak (−0.29) and moderate (−0.46) negative correlation coefficients, these results show that the serum albumin level, platelet count, and prothrombin time decrease significantly as the ratio of red increases (Figure 6).

Figure 3. Procedure for calculating the ratio of the red to the entire contrast-enhanced area of the liver parenchyma. From the obtained arrival time parametric images, the red area of the liver parenchyma and the entire contrast-enhanced area were calculated using ImageJ software to determine the ratio of red.

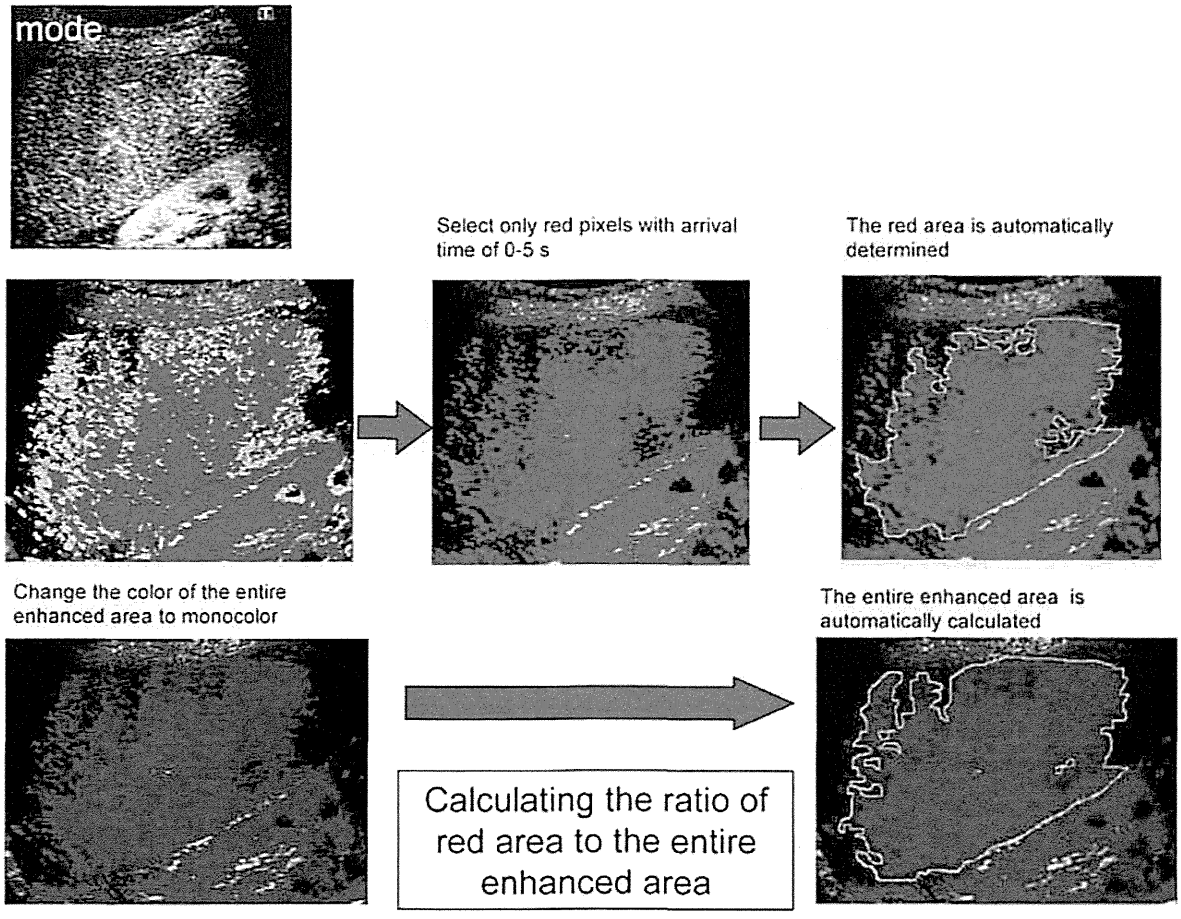

The optimal cutoff values (area under the ROC curve) for differentiating fibrosis stages between F0–F1 and F2 and higher and between F0–F3 and F4 were 18.3% (0.909) and 69.0% (0.962), respectively. The sensitivity and specificity for diagnosing the fibrosis stage by arrival time parametric imaging using the cutoff values were 0.971 and 0.657 for diagnosing stages F2 and higher and 0.889 and 0.918 for diagnosing stage F4, showing high sensitivity and specificity for the technique. Positive and negative predictive values were 73.9% and 95.8% at F2 and higher and 61.5% and 98.2% at F4 (Figures 7 and 8 and Table 3).

Discussion

Percutaneous liver biopsy is considered the reference standard for diagnosing liver fibrosis in chronic liver diseases such as hepatitis C.[7,8] However, liver biopsy is an invasive procedure and is associated with risk-posing complications, such as bleeding.[9] It is also disadvantageous in that it only enables evaluation of a local site in the liver.[10,11] As a noninvasive alternative to liver biopsy, sonographically based techniques, such as transient elastography (FibroScan; Echosens SA, Paris, France), real-time tissue elastography, and acoustic radiation force impulse, have recently been developed and applied for diagnosing liver fibrosis.[12–18] These techniques can still cause measurement errors depending on patient condition, such as ascites, or insufficient ultrasound penetration.[12,15,18]

Table 1. Individual and Mean Ratio of Red Values for Healthy Volunteers and Patients With Fibrosis

	Volunteers (n = 10)	F1 (n = 25)	F2 (n = 20)	F3 (n = 6)	F4 (n = 9)
Ratio, %	14.4	25.0	30.9	78.6	90.0
	12.5	46.7	32.7	65.1	98.8
	3.9	15.6	39.2	85.3	63.5
	7.3	26.9	36.5	40.1	83.5
	12.4	22.1	12.3	56.0	96.5
	13.2	6.0	54.2	54.5	77.9
	12.4	10.8	43.0		69.0
	21.1	31.3	73.4		83.7
	22.5	41.8	22.7		95.8
	17.5	30.7	24.1		
		6.5	60.3		
		19.4	84.6		
		10.5	38.1		
		12.5	18.3		
		16.4	86.5		
		8.7	20.6		
		22.6	19.2		
		36.3	21.9		
		16.3	21.5		
		12.2	31.4		
		3.1			
		15.7			
		5.4			
		16.4			
		8.1			
Mean	13.7	18.7	38.6	63.3	84.3

F indicates fibrosis stage.

We have previously shown that the contrast-enhanced liver-kidney blood flow contrast technique using Levovist can capture a change in the liver blood flow balance in chronic liver disease by comparing the enhancement pattern of the liver with that of the kidney, which is supplied exclusively by arteries.[5] The time interval between kidney enhancement and liver enhancement was significantly shortened as the disease stage advanced from normal to chronic hepatitis to cirrhosis. These findings suggested that as the disease stage advances toward cirrhosis, hepatic parenchymal blood flow is arterialized; ie, portal flow is decreased while rapid arterial flow is increased, and the enhancement pattern of the liver parenchyma becomes similar to that of the kidney. It was thus expected that this technique can be used as a noninvasive modality for diagnosing liver fibrosis. In the Levovist-based technique, enhancement patterns are obtained via a bubble destruction signal, which makes it difficult to continuously observe hepatic parenchymal blood flow for detailed analysis. In contrast, Sonazoid enables continuous observation of the enhancement pattern without the need for bubble destruction. We thus attempted to analyze the blood flow arrival time to the liver and kidney based on a time-intensity curve obtained by Sonazoid-enhanced sonography. The use of Sonazoid enabled a detailed evaluation of the degree of disease progression in chronic liver disease. However, because the time-intensity curve is a graph, it does not enable intuitive and easy interpretation of blood flow for everyone. It is also problematic that time-intensity curves can vary readily under different testing conditions, such as with different volumes and infusion rates of the contrast medium. We then assumed that arrival time parametric imaging, a technique for evaluating the blood flow arrival time, which can easily and clearly visualize contrast enhancement patterns on sonography in color, would be clinically more useful if it could also evaluate the degree of liver disease progression in chronic hepatitis C infection.

This study revealed that arrival time parametric imaging was correlated significantly and positively with the liver fibrosis stage and negatively with the serum albumin level, platelet count, and prothrombin time, showing the feasibility of arrival time parametric imaging–based evaluation of the degree of liver disease progression in chronic hepatitis C in-

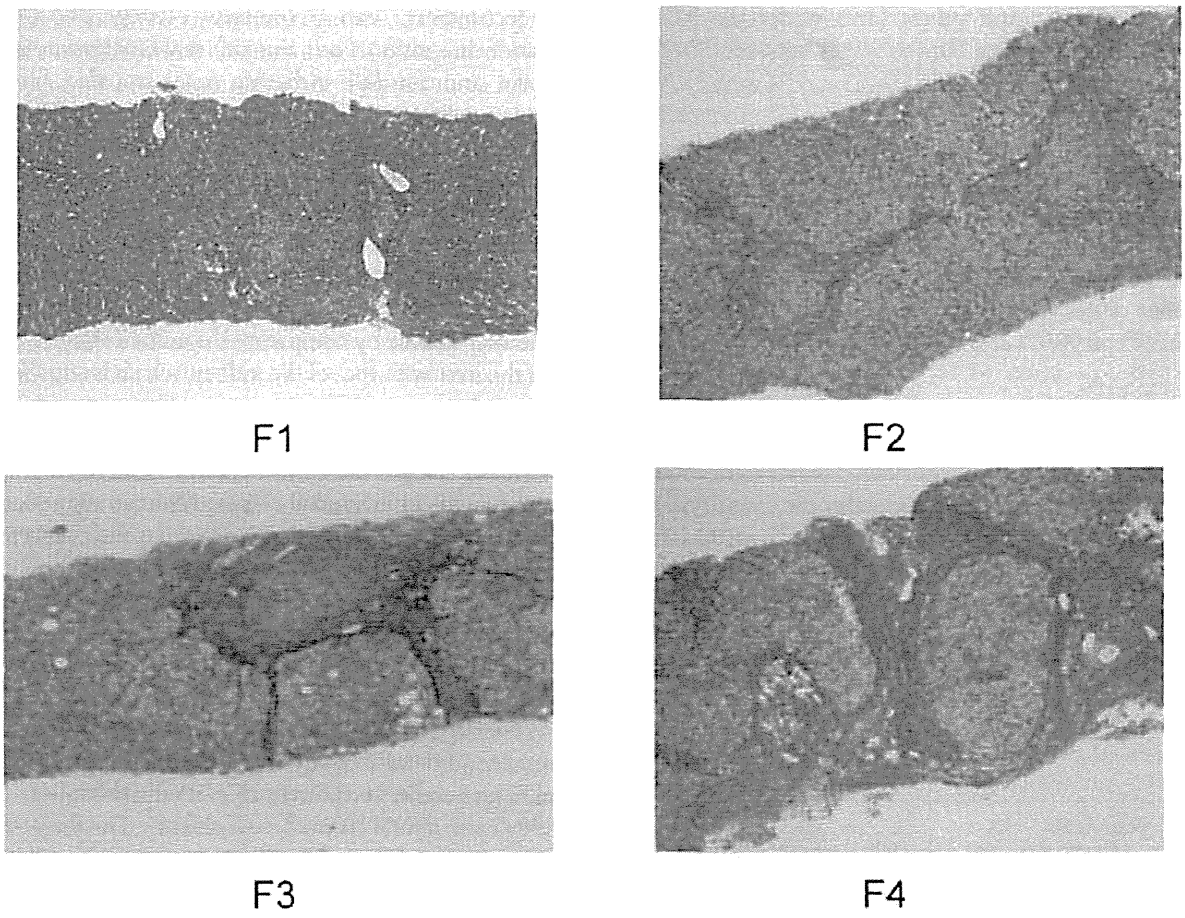

Figure 4. Pathologic findings of liver fibrosis (azan, original magnification ×4). Fibrosis was staged as follows: F1, portal fibrosis without septa; F2, portal fibrosis and few septa; F3, numerous septa without cirrhosis; and F4, cirrhosis.

Table 2. Characteristics of Patients and Healthy Volunteers

Characteristic	Patients (n = 60)	Volunteers (n = 10)
Male/female	34/26	6/4
Age, y	53 ± 12	63 ± 15
AST level, U/L	63.0 ± 47.5	12.0 ± 5.2
ALT level, U/L	70.5 ± 55.9	15.0 ± 4.0
Platelet count, × 10^4/μL	14.6 ± 6.0	21.1 ± 2.5
Total bilirubin, mg/dL	0.8 ± 0.3	0.9 ± 0.6
Prothrombin time, % of normal	92.8 ± 13.8	101.3 ± 11.2
Albumin, g/dL	4.0 ± 0.4	4.3 ± 0.3
Total cholesterol, mg/dL	161.4 ± 26.4	201.8 ± 37.1
F0	0	
F1	25	
F2	20	
F3	6	
F4	9	

Values are mean ± SD where applicable. ALT indicates alanine aminotransferase; AST, aspartate transaminase; and F, fibrosis stage.

Figure 5. Parameter analysis measured by arrival time parametric imaging for each fibrosis stage: box plots of each arrival time parametric imaging value corresponding to fibrosis stages F1–F4 and the healthy volunteer group (Control). The top and bottom of each box indicates the first and third quartiles. The length of the box represents the interquartile range within which 50% of values are located. The line through the middle of each box represents the median value. Control, n = 10; F1–F4, n = 60.

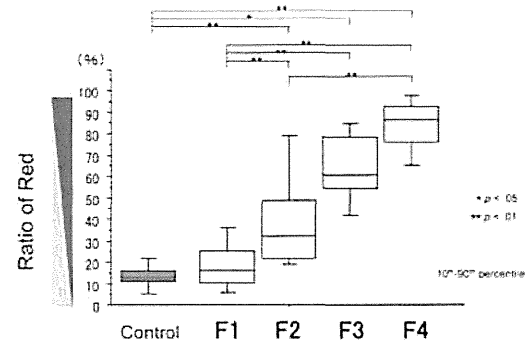

Figure 6. Correlation between blood examination and ratio of red parameters. **A**, The ratio of red correlated negatively with the albumin level. **B**, The ratio of red correlated negatively with the platelet count. **C**, The ratio of red correlated negatively with prothrombin time.

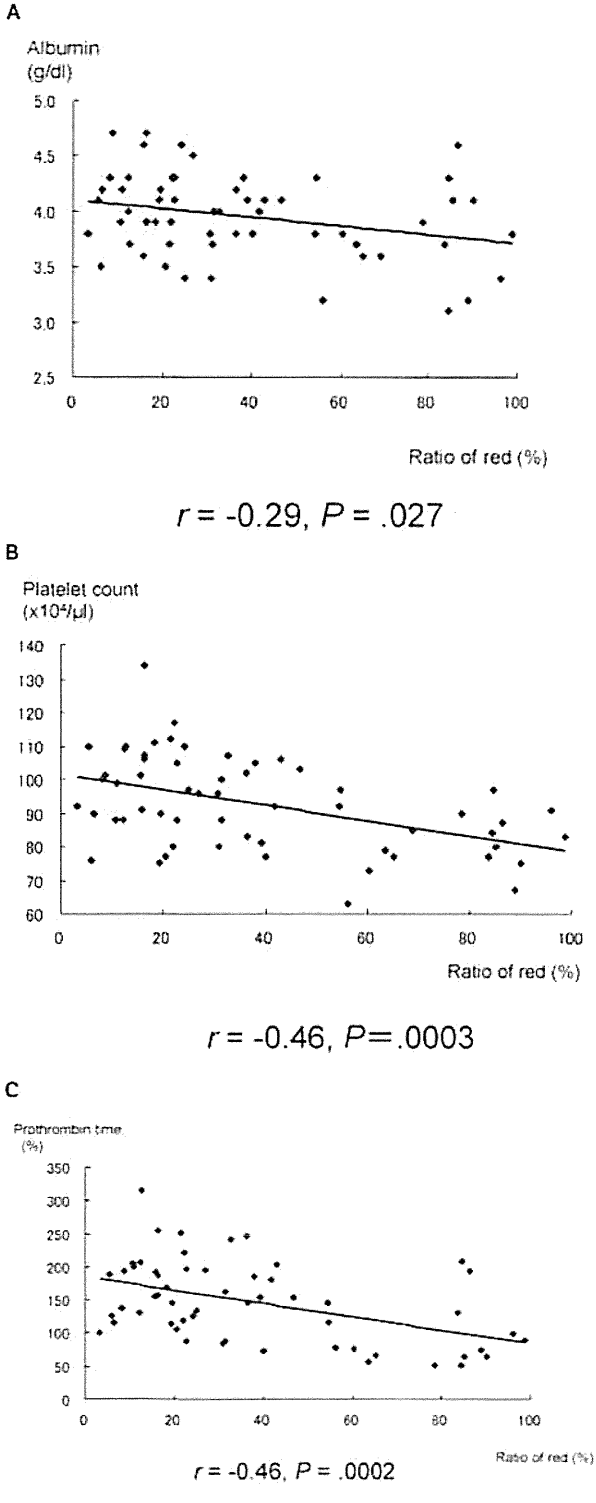

fection. However, strong correlations were not observed between the ratio of red and the serum albumin level, platelet count, and prothrombin time. This finding may have been attributable to the fact that the serum albumin level, platelet count, and prothrombin time are affected not only by hepatic blood flow but also by other complex factors, including splenomegaly and the nutritional state.

Compared to results obtained by the time-intensity curve, those obtained by arrival time parametric imaging were simple and easy to interpret. In addition, with this technique, you can present still images to a third person for explanation purposes. Such features make this technique clinically useful.

This technique involves visualization of the right hepatic lobe and right kidney via right intercostal scanning to determine the time interval between enhancement initiation in the liver and that in the kidney. It is thus likely that the technique captures blood flow information in the entire part of the right hepatic lobe and thus enables more accurate evaluation of the degree of disease progression than liver biopsy, which can only capture the condition of a local site of the liver.

The optimal cutoff values (area under the ROC curve) for differentiating fibrosis stages between F0–F1 and F2 and higher and between F0–F3 and F4 were 18.3% (0.909) and 69.0% (0.962), respectively. The sensitivity and specificity for diagnosing fibrosis stages by arrival time parametric imaging using the cutoff values were 0.971 and 0.657 for diagnosing stages F2 and higher and 0.889 and 0.918 for diagnosing stage F4, showing high sensitivity and specificity. These results suggest the clinical use-

Figure 7. Receiver operating characteristic curve for arrival time parametric imaging diagnosis of stage F2 liver fibrosis (area under curve = 0.909).

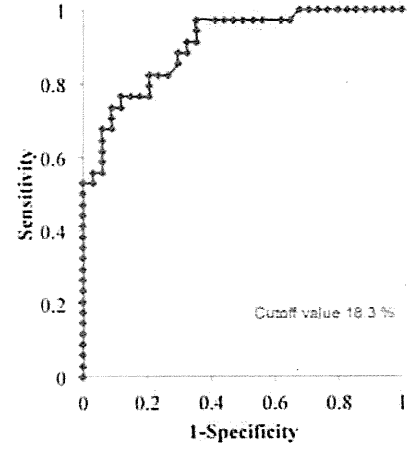

fulness of this technique because it may also be used to identify F4 patients, who are considered associated with a higher incidence of hepatocellular carcinoma than F0–F3 patients. The technique can also be used to estimate when to start interferon therapy, which is currently recommended for patients with F2 and higher stages in Japan.

The arrival time parametric imaging–based technique aims to visualize the difference between the blood flow arrival time to the liver and the kidney and is totally different from liver stiffness visualization/quantification techniques, such as transient elastography (FibroScan), real-time tissue elastography, and acoustic radiation force impulse. Arrival time parametric imaging is advantageous in that it can (1) capture the status of hepatic blood flow and (2) enable presentation of obtained data as completed, final still images to a third person to provide a clear explanation with color images. Such features make the technique highly clinically useful. The ability of arrival time parametric imaging to differentiate fibrosis stages between F0–F1 and F2 and higher and between F0–F3 and F4 was comparable to that of acoustic radiation force impulse[19] (91.4% sensitivity and 80.0% specificity for ≥F2 and 94.1% sensitivity and 86.8% specificity for F4), real-time tissue elastography[20] (84.1% sensitivity and 82.7% specificity for ≥F2 and 85.7% sensitivity and 82.9% specificity for F4), and transient elastography[21] (80.8% sensitivity and 80.3% specificity for ≥F2 and 91.7% sensitivity and 78.0% specificity for F4).

There were, however, several limitations to this study. The following diseases and conditions may affect the results of this method: heart diseases associated with possible alteration of the arrival time of the contrast agent to the liver, renal disorders associated with possible alterations of the kinetics of ultrasonic signals in the kidney, heavy drinking habits associated with possible changes in hemodynamics, the presence of extensive collateral circulation(s), and portal vein embolisms associated with possible disturbances of the balance between arterial and portal blood flow. Thus, patients with these diseases or conditions cannot be examined by this method. Furthermore, patients whose right hepatic lobe cannot be visualized by sonography, such as those with narrow intercostal spaces, as well as those who have difficulties holding their breath for 15 to 20 seconds, have to be excluded. Because Sonazoid, the contrast agent used in this method, contains an egg derivative, an egg allergy is a contraindication.

The cost of sonographic examination with Sonazoid is lower than that of magnetic resonance imaging with a contrast agent. The cost of Sonazoid-enhanced sonography is slightly higher than that of computed tomography with a contrast agent, but sonography has advantages over computed tomography such as no risk of exposure to radiation and portability of the system. Furthermore, another advantage is that sonography can be performed repeatedly to monitor changes in chronic hepatitis C lesions. Although sonography costs more than liver biopsy, patients in Japan must be hospitalized for liver biopsy, which is inconvenient. Moreover, liver biopsy carries a considerable risk of complications.

In conclusion, we evaluated patients with liver disease progression in chronic hepatitis C infection and revealed that the ratio of red correlates with the degree of liver fibrosis and liver function. Thus, this technique is potentially useful for determining the initiation timing of interferon therapy, assessing the efficacy of interferon therapy (alleviation of fibrosis), and predicting the onset of complications of portal hypertension (esophageal varices, splenomegaly, and ascites).

Figure 8. Receiver-operating characteristic curve for arrival time parametric imaging diagnosis of stage F4 liver fibrosis (area under curve = 0.962).

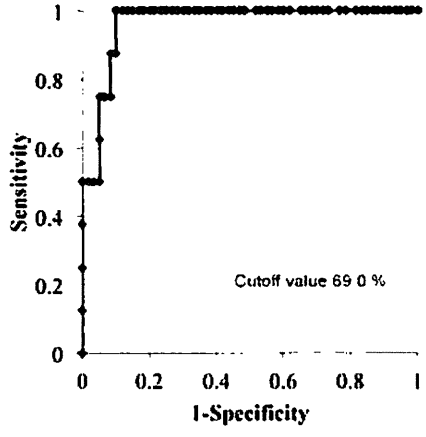

Table 3. Performance of Arrival Time Parametric Imaging for the Assessment of Histologic Fibrosis Stage in Patients With Chronic Liver Disease

Parameter	F≥2	F4
Cutoff ratio of red, %	18.3	69.0
PPV, %	73.9	61.5
NPV, %	95.8	98.2
Sensitivity, %	97.1	88.9
Specificity, %	65.7	91.8
AUC	0.909	0.962

AUC indicates area under the receiver operating characteristic curve; F, fibrosis stage; NPV, negative predictive value; and PPV, positive predictive value.

References

1. Kleber G, Steudel N, Behrmann C, et al. Hepatic arterial flow volume and reserve in patients with cirrhosis: use of intra-arterial Doppler and adenosine infusion. *Gastroenterology* 1999; 116:906–914.
2. Rocheleau B, Ethier C, Houle R, Huet PM, Bilodeau M. Hepatic artery buffer response following left portal vein ligation: its role in liver tissue homeostasis. *Am J Physiol* 1999; 277:G1000–G1007.
3. Leen E, Goldberg JA, Anderson J, et al. Hepatic perfusion changes in patients with liver metastases: comparison with those patients with cirrhosis. *Gut* 1993; 34:554–557.
4. Lautt WW. Mechanism and role of intrinsic regulation of hepatic arterial blood flow: hepatic arterial buffer response. *Am J Physiol* 1985; 249:G549–G556.
5. Fujita Y, Watanabe M, Sasao K, et al. Investigation of liver parenchymal flow using contrast-enhanced ultrasound in patients with alcoholic liver disease. *Alcohol Clin Exp Res* 2004; 28(suppl):169S–173S.
6. Bedossa P, Poynard T. An algorithm for the grading of activity in chronic hepatitis C. The Metavir Cooperative Study Group. *Hepatology* 1996; 24:289–293.
7. Desmet VJ, Gerber M, Hoofnagle JH, Manns M, Scheuer PJ. Classification of chronic hepatitis: diagnosis, grading and staging. *Hepatology* 1994; 19:1513–1520.
8. Ishak K, Baptista A, Bianchi L, et al. Histological grading and staging of chronic hepatitis. *J Hepatol* 1995; 22:696–699.
9. Bravo AA, Sheth SG, Chopra S. Liver biopsy. *N Engl J Med* 2001; 344: 495–500.
10. Bedossa P, Dargere D, Paradis V. Sampling variability of liver fibrosis in chronic hepatitis C. *Hepatology* 2003; 38:1449–1457.
11. Colloredo G, Guido M, Sonzogni A, Leandro G. Impact of liver biopsy size on histological evaluation of chronic viral hepatitis: the smaller the sample, the milder the disease. *J Hepatol* 2003; 39:239–244.
12. Fraquelli M, Rigamonti C, Casazza G, et al. Reproducibility of transient elastography in the evaluation of liver fibrosis in patients with chronic liver disease. *Gut* 2007; 56:968–973.
13. Verveer C, de Knegt RJ. Non-invasive measurement of liver fibrosis: application of the FibroScan in hepatology. *Scand J Gastroenterol Suppl* 2006; 243:85–88.
14. Foucher J, Chanteloup E, Vergniol J, et al. Diagnosis of cirrhosis by transient elastography (FibroScan): a prospective study. *Gut* 2006; 55:403–408.
15. Kanamoto M, Shimada M, Ikegami T, et al. Real time elastography for noninvasive diagnosis of liver fibrosis. *J Hepatobiliary Pancreat Surg* 2009; 16:463–467.
16. Tatsumi C, Kudo M, Ueshima K, et al. Noninvasive evaluation of hepatic fibrosis using serum fibrotic markers, transient elastography (FibroScan) and real-time tissue elastography. *Intervirology* 2008; 51(suppl 1):27–33.
17. Nightingale K, McAleavey S, Trahey G. Shear-wave generation using acoustic radiation force: in vivo and ex vivo results. *Ultrasound Med Biol* 2003; 29:1715–1723.
18. Kettaneh A, Marcellin P, Douvin C, et al. Features associated with success rate and performance of FibroScan measurements for the diagnosis of cirrhosis in HCV patients: a prospective study of 935 patients. *J Hepatol* 2007; 46:628–634.
19. Takahashi H, Ono N, Eguchi Y, et al. Evaluation of acoustic radiation force impulse elastography for fibrosis staging of chronic liver disease: a pilot study. *Liver Int* 2010; 30:538–545.
20. Morikawa H, Fukuda K, Kobayashi S, et al. Real-time tissue elastography as a tool for the noninvasive assessment of liver stiffness in patients with chronic hepatitis C. *J Gastroenterol* 2011; 46:350–358.
21. Nitta Y, Kawabe N, Hashimoto S, et al. Liver stiffness measured by transient elastography correlates with fibrosis area in liver biopsy in patients with chronic hepatitis C. *Hepatol Res* 2009; 39:675–684.

Journal of Gastroenterology and Hepatology

JGHF

doi:10.1111/jgh.12181

HEPATOLOGY

Noninvasive evaluation of hepatic fibrosis in hepatitis C virus-infected patients using ethoxybenzyl-magnetic resonance imaging

Shunsuke Nojiri, Atsunori Kusakabe, Kei Fujiwara, Noboru Shinkai, Kentaro Matsuura, Etsuko Iio, Tomokatsu Miyaki and Takashi Joh

Department of Gastroenterology and Metabolism, Nagoya City University Graduate School of Medical Sciences, Nagoya, Aichi, Japan

Key words
EOB-MRI, hepatic fibrosis, noninvasive methods.

Accepted for publication 4 February 2013.

Correspondence
Shunsuke Nojiri, Department of Gastroenterology and Metabolism, Nagoya City University Graduate School of Medical Sciences, Kawasumi 1, Mizuho-cho, Mizuho-ku, Nagoya, Aichi 467-8601, Japan.
Email: snojiri@med.nagoya-cu.ac.jp

Conflicts of interest: None.

Authors' contributions: SN and JT analyzed the data. KF, AK, NS, KM, EI, and TM collected MRI data and performed liver biopsies.

Abstract

Background and Aims: Liver biopsy is the gold standard test to determine the grade of fibrosis, but there are associated problems. Because gadolinium-ethoxybenzyl-diethylenetriamine pentaacetic acid is secreted partially in hepatocytes and bile, it is possible that ethoxybenzyl-magnetic resonance imaging (EOB-MRI) correlates with liver function and liver fibrosis. The aim of this study was to compare the fibrosis seen in liver biopsy samples to the signal intensity of the hepatobiliary phase measured on EOB-MRI in hepatitis C virus (HCV)-infected patients.

Methods: Two hundred twenty-four (estimation 149, validation 75) HCV-infected patients with histologically proven liver tissue who underwent EOB-MRI were studied. Overall, fibrosis staging was 15/24/19/46/45 for F0/F1/F2/F3/F4, respectively. A 1.5-Tesla magnetic resonance system was used, and the regions of interest of the liver were measured. Four methods were used: (i) relative enhancement: (post-enhanced signal intensity [SI] – pre-enhanced intensity)/pre-enhanced intensity; (ii) liver-to-intervertebral disk ratio (LI): post-enhanced (liver SI/interdisc SI)/pre-enhanced (liver SI/inter disc SI); (iii) liver-to-muscle ratio: post-enhanced (liver SI/muscle SI)/pre-enhanced (liver SI/muscle SI); and (iv) liver-to-spleen ratio: post-enhanced (liver SI/spleen SI)/pre-enhanced (liver SI/spleen SI).

Results: To discriminate F0-1 *versus* F2-4 or F0-2 *versus* F3-4 or F0-3 *versus* F4, LI at 25 min (LI25) had the highest area under receiver operating characteristic (0.88, 0.87, and 0.87, respectively) in these four methods and also in the validation set.

Conclusion: LI at 25 min seems to be a useful method to determine the staging of fibrosis as a non-invasive method in HCV-infected hepatitis or cirrhosis patients.

Introduction

Chronic hepatitis C is the most common cause of cirrhosis in the world. The most appropriate treatment is interferon and ribavirin combination therapy, with efficacy of up to 70%. If this therapy is not effective, patients will progress to cirrhosis 25–30 years after infection.[1] Hepatitis C virus (HCV)-related cirrhosis is associated with an extremely high risk of hepatocellular carcinoma (HCC) development.[2–4] Treatment of HCC at an early stage has a good prognosis,[5–7] but advanced fibrosis increases the risk of carcinogenesis,[3] so it is important to know its fibrotic stage in outpatients. Liver biopsy is the gold standard test to determine the grade of fibrosis, but there are associated problems, such as sample error and severe complications.[8–10] Previously, methods using usual laboratory data have been reported to predict significant fibrosis or cirrhosis in patients, such as Forn's score:[11] platelet count, gamma-glutamyl transpeptidase, total cholesterol, and age; the FibroIndex:[12] platelet count, aspartate aminotransferase (AST), and gamma globulin; the Lok index:[13] platelet, prothrombin time (PT) (international normalized ratio), AST, and alanine aminotransferase (ALT); and the AST-to-platelet ratio index (APRI):[14] AST and platelet count. In recent years, several non-invasive methods have been reported, such as transient elastography (Fibroscan, Echosens, Paris, France),[15] magnetic resonance (MR) elastography,[16] and acoustic radiation force impulse.[17] These methods require special equipment and are expensive, so newly developed techniques that can be used in general hospitals and estimate liver parenchyma are needed. Gadolinium-ethoxybenzyl-diethylenetriamine pentaacetic acid (Gd-EOB-DTPA) is an agent that is widely used to detect HCC or metastatic liver tumor.[18] This is a liver-specific agent with 50% uptake in the liver. It partially accumulates in hepatocytes and is excreted into bile, so it is possible that ethoxybenzyl-magnetic resonance imaging (EOB-MRI) correlates with liver function and liver fibrosis. The aim of this

study was to compare the fibrosis seen in liver biopsy samples with the signal intensity (SI) of the hepatobiliary phase measured on EOB-MRI and differentiate HCV-infected patients with significant fibrosis (F2-4) from those without significant fibrosis (F0,1) or with extended fibrosis (F3,4) from the others (F0-2), or cirrhosis (F4) from non-cirrhosis followed by determining the best measurement method using EOB-MRI.

Patients and methods

Patients. Between August 2008 and July 2011, we studied 246 HCV-infected patients with histologically proven liver tissues who underwent EOB-MRI. Clinical data and EOB-MRI were obtained within 1 month before the liver biopsy or operation. HCV infection was defined by a positive anti-HCV test and detection of HCV-RNA in either a quantitative or qualitative assay. Exclusion criteria were infection with hepatitis B or human immunodeficiency viruses, alcohol abuse, numerous liver tumors, and previous partial splenic arterial embolization (PSE) or splenectomy. Nine patients were excluded due to inadequate biopsy specimens for the fibrosis stage, two patients with HBV infection, five patients with high alcohol consumption, three who had undergone PSE, one who had undergone splenectomy, and two patients because of numerous liver tumors. Finally, 224 patients were enrolled in the study. Data were randomly split almost two to one for model estimation and model validation: 149 patients (male 99, female 50, mean age 71 ± 8) for estimation and 75 (male 45, female 30, mean age 65 ± 13) for validation.

Histological staging. Liver tissue was obtained by percutaneous needle biopsy using a 14–16G biopsy needle or from liver specimens resected during surgery. Biopsy specimens were stained with hematoxylin and eosin, and Masson's trichrome staining. Liver fibrosis was evaluated according to the METAVIR scoring system:[10] F0, no fibrosis; F1, portal fibrosis without septa; F2, few septa; F3, numerous septa without cirrhosis; F4, cirrhosis. One pathologist, who was unaware of the patient characteristics, assessed and scored the specimens. Overall, fibrosis staging for estimation was 15(3)/24(1)/19(0)/46(2)/45(2) for F0/F1/F2/F3/F4, respectively, and the samples for validation were 11(2)/15(0)/12(1)/20(1)/17(1) for F0/F1/F2/F3/F4, respectively; () is surgical resection.

MRI techniques. We used a 1.5-Tesla MR system (PHILIPS Co., Amsterdam, the Netherlands); 0.025 mmol/kg bodyweight gadoxetate disodium was injected intravenously, and quantitative measurements were conducted using unenhanced and gadoxetate disodium-enhanced imaging at 20, 35, 70, and 180 s. Hepatobiliary phases at 15, 20, and 25 min were obtained. Imaging parameters were as follows: repetition time/echo time = 4.17/2.05 ms. Then, 1- to 2-cm^2 regions of interest of the mean SI value of the liver were measured for each MR image to calculate the means of three different regions (right anterior, right posterior, and left lateral segment) of the liver devoid of large vessels or prominent artifacts (Fig. 1a). We calculated MR enhancement with four different methods: (i) relative enhancement (RE) was calculated using the following equation: (post-enhanced SI—pre-enhanced SI)/pre-enhanced SI; (ii) using the liver-to-muscle (paraspinal muscles) SI (LMSI), liver SI/muscle SI, we calculated the post-enhanced LMSI/pre-enhanced LMSI (described as LM); (iii) using the liver-to-intervertebral disk SI (LISI), liver SI/intervertebral disk SI, we calculated the post-enhanced LISI/pre-enhanced LISI (described as LI); (iv) using the liver-to-spleen SI (LSSI), liver SI/spleen SI, we calculated the post-enhanced LSSI/pre-enhanced LSSI (described as LS). We compared several predictive methods

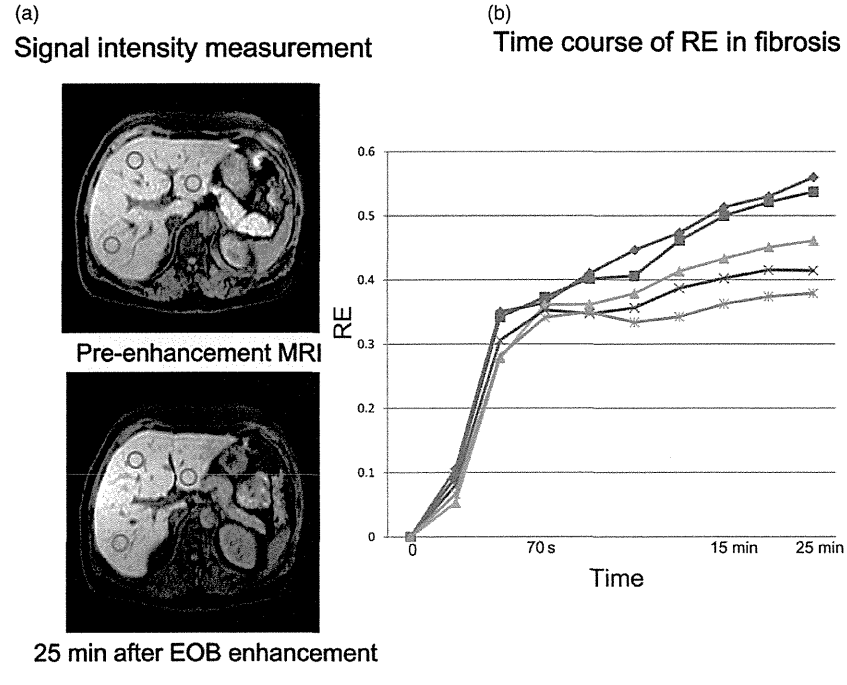

Figure 1 (a) One- to two-squared centimeter regions of interest of the mean signal intensity value of the liver were measured for each magnetic resonance image (MRI) to calculate the means of three different regions of the liver devoid of large vessels or prominent artifacts. (b) Time-course of relative enhancement (RE) after gadolinium-ethoxybenzyl (EOB)-diethylenetriamine pentaacetic acid injection. After EOB injection, relative enhancement increased gradually up to 25 min. RE of F0 and F1 was significantly higher than that of F2 at 15, 20, and 25 min. (—◆—) F0 (n = 15); (—■—) F1 (n = 24); (—▲—) F2 (n = 19); (—✕—) F3 (n = 46); (—✳—) F4 (n = 44).

of fibrosis published previously (Forn's score, FibroIndex, APRI, Lok index). Blood tests were performed in the hospital laboratories of the participating clinical centers. Age, sex, AST, ALT, albumin, total bilirubin, and platelet counts were examined, and the PT was measured as a percentage of the daily internal control. The diagnostic value of the MRI was assessed by calculating the areas under the receiver operating characteristic (ROC) curves. An area under the curve of 1.0 is characteristic of an ideal test, whereas 0.5 indicates a test of no diagnostic value.[19] The best models derived from the categorical variables were compared by the χ^2 or Fisher's exact test, whereas continuous variables were compared with Student's *t* test. Correlation was evaluated by the Spearman correlation coefficient. A two-sided *P* value of less than 0.05 was considered significant. Diagnostic accuracy was calculated by sensitivity, specificity, and positive and negative predictive values, considering significant fibrosis as the disease. The best cut-off points were selected from the ROC curve to identify the presence and absence of significant fibrosis. A representative cut-off point was determined by calculating the maximum sensitivity and specificity, and comparing their accuracy.

Results

Patient characteristics. A total of 224 patients were examined who had undergone liver biopsy.

The index was constructed with data from 149 patients (estimation set) and 75 patients (validation set). Patient characteristics at the time of liver biopsy are shown in Table 1. There were no significant differences between the estimation and validation sets in any clinical or biochemical variable or fibrosis stage.

Table 1 Baseline characteristics of 224 patients with chronic hepatitis C at the time of liver biopsy: comparison of the estimation and validation groups

Variable	All patients (*n* = 224)	Estimation group (*n* = 149)	Validation group (*n* = 75)	*P* value
Age	67 ± 12	71 ± 8	65 ± 13	ns
Male (M/F)	144/80	99/50	45/30	ns
AST (U/L)	48 ± 26	49 ± 27	45 ± 24	ns
ALT (U/L)	45 ± 36	44 ± 31	48 ± 45	ns
Gamma-gl (g/dL)	1.9 ± 0.52	1.9 ± 0.54	1.8 ± 0.52	ns
Gamma-GT (IU/L)	70.6 ± 87	77.5 ± 98	56.8 ± 56	ns
T.Bil (mg/dL)	0.9 ± 0.4	0.9 ± 0.4	0.9 ± 0.4	ns
PT (%)	87.9 ± 14.9	86.6 ± 15.0	90.6 ± 15.0	ns
Platelet (× 10^3/μL)	146 ± 66	138 ± 66	148 ± 66	ns
Stage of fibrosis				
F0	26 (11.6%)	15 (10.1%)	11 (14.7%)	ns
F1	39 (17.4%)	24 (16.1%)	15 (20.0%)	
F2	31 (13.8%)	19 (12.7%)	12 (16.0%)	
F3	66 (29.4%)	46 (30.9%)	20 (26.7%)	
F4	62 (27.7%)	45 (30.2%)	17 (22.7%)	

P values are for comparisons between the estimation set and the validation set.

ALT, alanine aminotransferase; AST, aspartate aminotransferase; gl, globulin; GT, glutamyl transpeptidase; ns, not significant; PT, prothrombin time; T.Bil, total bilirubin.

Time-course of RE in fibrosis. After EOB injection, RE increased rapidly for the first 35 s and gradually increased until 25 min (Fig. 1b). RE of F0 or F1 was significantly higher than that of F2 at 15, 20, and 25 min.

Because, at any stage (F0-F4), 25-min RE (RE25) was higher than 15-min RE (RE15) and 20-min RE (RE20) was between RE15 and RE25, we considered using 25-min data as the best method to obtain the most significant accuracy. We therefore decided to adopt 25-min data in this study, although the international consensus for the hepatobiliary phase is 20-min post-contrast.

Correlation of MRI enhancement in hepatobilialy phase and histological findings. Figure 2 shows box plots of several biochemical fibrosis indexes and several MRI fibrosis indexes. On MRI, the mean contrast enhancement index constantly decreased as the fibrosis stage progressed to a higher stage. Changes in the histological fibrosis stage correlated with changes in RE at 25 min: RE25 ($r = -0.478$); LM at 25 min: LM25 ($r = -0.463$); LI at 25 min: LI25 ($r = -0.661$); LS at 25 min: LS25 ($r = -0.376$); Forn's Index ($r = 0.551$); FibroIndex ($r = 0.6$); Lok index ($r = 0.561$); and APRI ($r = 0.480$) ($P < 0.001$).

Overall diagnostic performance of MRI enhancement and serum markers. ROC curves were used for evaluating the overall diagnostic performance of several MRI indexes for different degrees of fibrosis (Estimation: Fig. 3 for F0-F1 *versus* F2-F4, F0-F2 *versus* F3-F4, and F0-3 *versus* F4, Validation: Fig. 4 for F0-F1 *versus* F2-F4, F0-F2 *versus* F3-F4, and F0-3 *versus* F4).

Table 2 shows the areas under ROC scores of MRI indexes, Forn's score, APRI, FibroIndex, and Lok index for different degrees of fibrosis. For discriminating F0-1 from F2-4, area under receiver operating characteristics (AUROCs) were LI25 (0.88), LS25 (0.77), RE25 (0.83), LM25 (0.83), Forn's Index (0.82), APRI (0.79), FibroIndex (0.87), and Lok index (0.83). For discriminating F0-2 from F3, 4, AUROCs were LI25 (0.87), LS25 (0.72), RE25 (0.81), LM25 (0.75), Forn's Index (0.80), APRI (0.79), FibroIndex (0.85), and Lok index (0.82). For discriminating F0-3 from F4, AUROCs were LI25 (0.87), LS25 (0.69), RE25 (0.74), LM25 (0.78), Forn's Index (0.75), APRI (0.73), FibroIndex (0.84), and Lok index (0.79). In the MRI enhancement index, LI25 had the highest value of AUROC for discriminating significant, extensive fibrosis, and cirrhosis, and this was almost the same or higher than serum markers such as the FibroIndex and Forn's score. The only significant difference was observed between LI25 and LS25 for the diagnosis of cirrhosis ($P < 0.05$) on estimation. A significant difference was also observed between LI25 and LS15 or LM15 for the diagnosis of extensive fibrosis ($P < 0.05$) (data not shown).

Table 3 shows AUROC curves scores for different degrees of fibrosis on validation. For discriminating F0, 1 from F2-4, AUROCs were LI25 (0.85), LS25 (0.75), RE25 (0.83), LM25 (0.71), Forn's Index (0.83), APRI (0.80), FibroIndex (0.84), and Lok index (0.80). For discriminating F0-2 from F3, 4, AUROCs were LI25 (0.85), LS25 (0.72), RE25 (0.83), LM25 (0.73), Forn's Index (0.83), APRI (0.80), FibroIndex (0.84), and Lok index (0.78). For discriminating F0-3 from F4, AUROCs were LI25

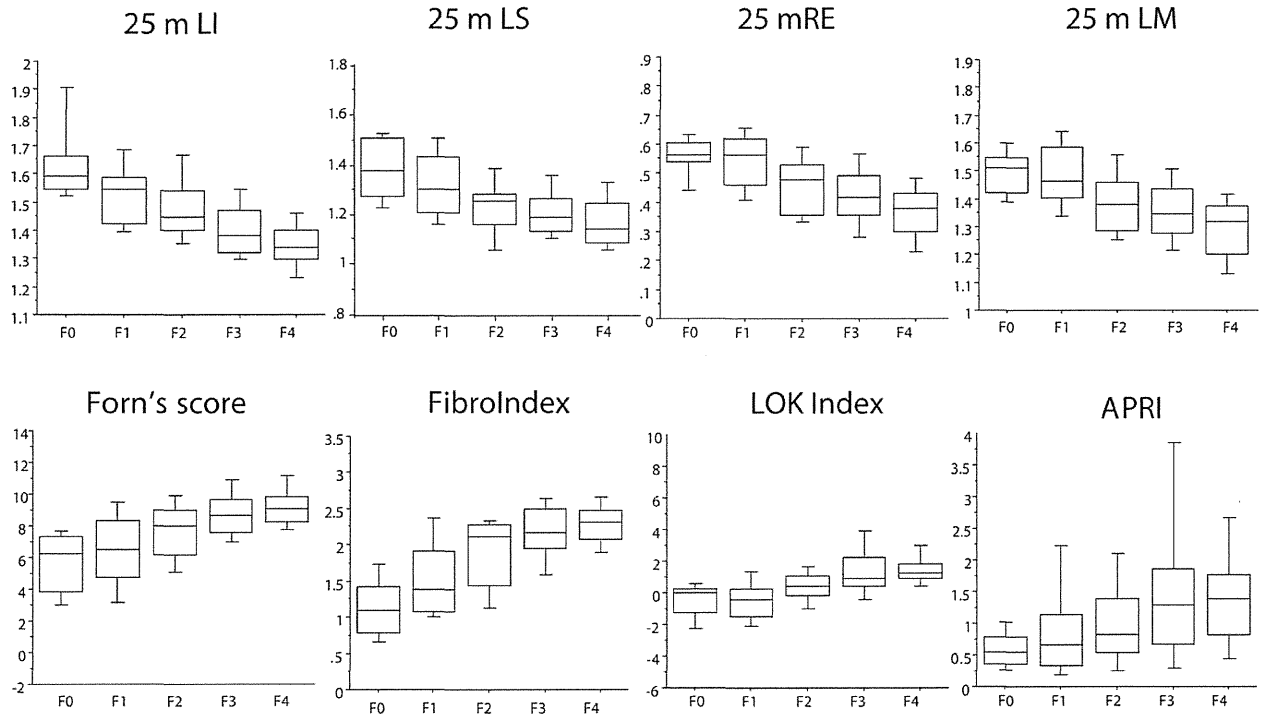

Figure 2 Scores according to METAVIR fibrosis stages. The top and bottom of each box are the 25th and 75th percentiles, respectively. The line through the box is the median, and the error bars are the 5th and 95th percentiles. Spearman correlation coefficients were as follows: 25 m relative enhancement (RE), $r = -0.478$; 25 m liver-to-muscle ratio (LM), $r = -0.463$; 25 m liver-to-intervertebral disk ratio (LI), $r = -0.661$; 25 m liver-to-spleen ratio (LS), $r = -0.376$; Forn's score, $r = 0.551$; FibroIndex, $r = 0.600$; Lok index, $r = 0.561$; aspartate aminotransferase-to-platelet ratio index (APRI), $r = 0.480$, $P < 0.001$ for each correlation test.

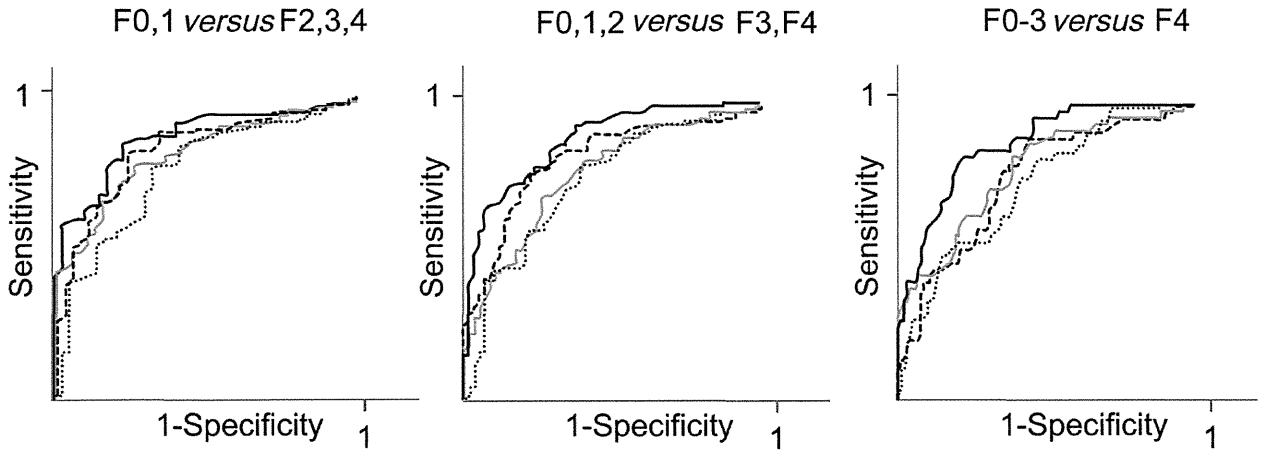

Figure 3 Receiver operating characteristic curve testing ability of the various methods to discriminate METAVIR fibrosis stage F0/F1 from F2/F3/F4, F0/F1/F2 from F3/F4, and F0-3 from F4 at 25 min in the estimation set. (——) liver-to-intervertebral disk ratio (LI); (·····) liver-to-spleen ratio (LS); (- - - - -) relative enhancement (RE); (——) liver-to-muscle ratio (LM).

(0.86), LS25 (0.67), RE25 (0.82), LM25 (0.82), Forn's Index (0.74), APRI (0.78), FibroIndex (0.83), and Lok index (0.82).

Also, in the validation group as well as the estimation group, in the MRI enhancement index, LI25 had the highest value of AUROC for discriminating significant, extensive fibrosis, and cirrhosis, and this was almost the same or higher than serum markers such as the FibroIndex and Forn's score as well as the estimation group.

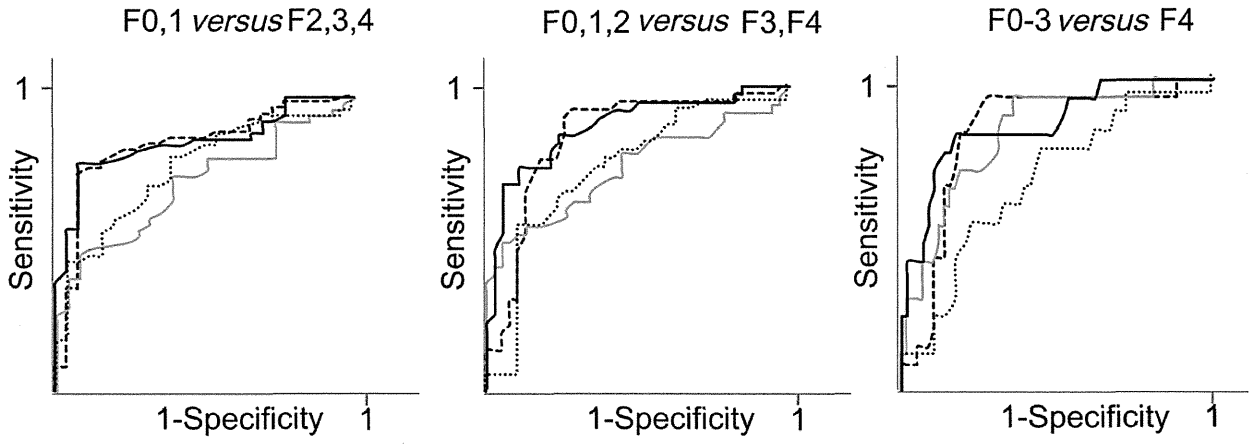

Figure 4 Receiver operating characteristic curve testing ability of the various methods to discriminate METAVIR fibrosis stage F0/F1 from F2/F3/F4, F0/F1/F2 from F3/F4, and F0-3 from F4 at 25 min in the validation set. (——) liver-to-intervertebral disk ratio (LI); (·····) liver-to-spleen ratio (LS); (- - - - -) relative enhancement (RE); (——) liver-to-muscle ratio (LM).

Table 2 Comparison of AUROC of scores for identifying significant (F2/F3/F4), extensive (F3/F4) fibrosis or cirrhosis (F4) on estimation

	F0F1 *versus* F2-F4			F0-F2 *versus* F3F4			F0-F3 *versus* F4		
	AUROC	SD	95% CI	AUROC	SD	95% CI	AUROC	SD	95% CI
LI	0.88	0.03	0.82–0.94	0.87	0.02	0.83–0.91	0.87†	0.02	0.83–0.91
LS	0.77	0.02	0.73–0.81	0.72	0.02	0.68–0.76	0.69	0.02	0.65–0.73
RE	0.83	0.03	0.77–0.89	0.81	0.02	0.77–0.85	0.74	0.02	0.70–0.78
LM	0.83	0.03	0.77–0.89	0.75	0.02	0.71–0.79	0.78	0.02	0.74–0.82
Forn's score	0.82	0.02	0.78–0.86	0.8	0.02	0.76–0.84	0.75	0.02	0.71–0.79
APRI	0.79	0.03	0.73–0.85	0.79	0.03	0.73–0.85	0.73	0.02	0.69–0.77
FibroIndex	0.87	0.03	0.81–0.93	0.85	0.02	0.81–0.89	0.84	0.02	0.80–0.88
Lok Index	0.83	0.02	0.79–0.87	0.82	0.02	0.78–0.86	0.79	0.02	0.75–0.83

†Significant differences were observed between LI25 and LS25 for diagnosis of cirrhosis ($P < 0.05$).
APRI, aspartate aminotransferase-to-platelet ratio index; AUROC, area under receiver operating characteristic; CI, confidence interval; LI, liver-to-intervertebral disk ratio; LM, liver-to-muscle ratio; LS, liver-to-spleen ratio; RE, relative enhancement; SD, standard deviation.

Table 3 Comparison of AUROC of scores for identifying significant (F2/F3/F4), extensive (F3/F4) fibrosis, or cirrhosis (F4) on validation

	F0F1 *versus* F2-F4			F0-F2 *versus* F3F4			F0-F3 *versus* F4		
	AUROC	SD	95% CI	AUROC	SD	95% CI	AUROC	SD	95% CI
LI	0.85	0.02	0.81–0.87	0.85	0.02	0.82–0.90	0.86	0.02	0.82–0.90
LS	0.75	0.02	0.71–0.79	0.72	0.02	0.68–0.76	0.67	0.02	0.63–0.71
RE	0.83	0.03	0.77–0.89	0.83	0.02	0.79–0.87	0.82	0.02	0.78–0.86
LM	0.71	0.02	0.67–0.75	0.73	0.02	0.69–0.77	0.82	0.02	0.78–0.86
Forn's score	0.83	0.03	0.77–0.89	0.83	0.02	0.79–0.87	0.74	0.02	0.70–0.78
APRI	0.8	0.03	0.74–0.86	0.8	0.03	0.74–0.86	0.78	0.03	0.72–0.84
FibroIndex	0.84	0.03	0.78–0.90	0.84	0.03	0.78–0.90	0.83	0.02	0.79–0.87
Lok Index	0.8	0.02	0.76–0.84	0.78	0.02	0.74–0.82	0.82	0.02	0.78–0.86

No significant differences were observed.
APRI, aspartate aminotransferase-to-platelet ratio index; AUROC, area under receiver operating characteristic; CI, confidence interval; LI, liver-to-intervertebral disk ratio; LM, liver-to-muscle ratio; LS, liver-to-spleen ratio; RE, relative enhancement; SD, standard deviation.

Sensitivity, specificity, and positive and negative predictive values (Tables 4 and 5). Based on the ROC, two cut-off values were chosen to identify the absence (≧ 1.62, 1.55, and 1.47) and presence (≦ 1.38, 1.38, and 1.315) of significant and extent fibrosis and cirrhosis, respectively. Applying the higher cut-off (≧ 1.62), 9 (23%) of the 39 patients without significant fibrosis in the liver biopsy were correctly identified (number of data not described in the Table). The presence of

Table 4 Sensitivity, specificity, and predictive value of scores according to different cut-offs for diagnosis of significant, extensive fibrosis and cirrhosis on estimation

	Significant (F2-F4)						Extent (F3,4)						Cirrhosis (F4)					
	Cut-off	Sen	Spe	PPV	NPV	Accuracy	Cut-off	Sen	Spe	PPV	NPV	Accuracy	Cut-off	Sen	Spe	PPV	NPV	Accuracy
LI25	≧ 1.62	96.4	23.1	77.9	69.2	0.77	≧ 1.55	96.7	46.6	73.9	90	0.77	≧ 1.47	95.6	52.9	46.7	96.5	0.66
	≦ 1.38	50.9	97.4	98.3	41.3	0.66	≦ 1.38	59.3	94.8	94.7	59.8	0.73	≦ 1.315	40	94.2	75	78.4	0.78
	≦ 1.55	93.6	60	86.9	85.2	0.86	≦ 1.51	90.1	62.1	78.8	80	0.79	≦ 1.38	77.8	80.8	63.6	89.4	0.8
Forn's score	≧ 5.3	95.5	43.6	82.7	77.3	0.82	≧ 7.15	43.1	93.4	56.9	77.3	0.79	≧ 9.1	51.1	76.9	48.9	78.4	0.69
APRI	≧ 0.85	81.8	66.7	87.4	56.5	0.78	≧ 0.85	86.8	58.6	76.7	73.9	0.76	≧ 1.1	93.3	56.8	48.3	95.2	0.68
FibroIndex	≧ 1.74	87.3	79.5	92.3	68.9	0.85	≧ 1.77	92.3	65.5	80.8	84.4	0.82	≧ 2.14	77.8	71.2	53.8	88.1	0.73
Lok Index	≧ 0.25	81	76.9	90.9	60	0.81	≧ 0.55	76.9	81	86.4	69.1	0.79	≧ 0.95	82.2	73.1	56.9	90.5	0.76

APRI, aspartate aminotransferase-to-platelet ratio index; LI, liver-to-intervertebral disk ratio; NPV, negative predictive value; PPV, positive predictive value; Sen, sensitivity; Spe, specificity.

Table 5 Sensitivity, specificity, and predictive value of scores according to different cut-offs for diagnosis of significant, extensive fibrosis and cirrhosis on validation

	Significant (F2-F4)						Extent (F3,4)						Cirrhosis (F4)					
	Cut-off	Sen	Spe	PPV	NPV	Accuracy	Cut-off	Sen	Spe	PPV	NPV	Accuracy	Cut-off	Sen	Spe	PPV	NPV	Accuracy
LI25	≧ 1.62	85.7	38.5	72.4	58.8	0.69	≧ 1.55	86.8	62.2	70.2	82.1	0.75	≧ 1.47	82.4	67.2	42.4	92.9	0.71
	≦ 1.38	44.9	96.2	95.7	48.1	0.63	≦ 1.38	51.4	94.7	90.5	66.7	0.73	≦ 1.315	47.1	93.1	66.7	85.7	0.82
	≦ 1.55	77.6	88.5	92.7	67.9	0.81	≦ 1.51	83.8	73.7	75.6	82.4	0.79	≦ 1.38	76.5	86.2	61.9	92.6	0.84
Forn's score	≧ 5.3	89.8	53.8	78.6	73.7	0.77	≧ 7.15	70.3	73.7	72.2	71.8	0.72	≧ 9.1	412	87.9	50	83.6	0.77
APRI	≧ 0.85	79.6	73.1	84.8	65.5	0.77	≧ 0.85	83.8	65.8	70.5	80.6	0.75	≧ 1.1	82.4	60.3	37.8	92.1	0.65
FibroIndex	≧ 1.74	79.6	76.9	86.7	66.7	0.79	≧ 1.77	83.8	76.3	77.5	82.9	0.8	≧ 2.14	70.6	77.6	48	90	0.76
Lok Index	≧ 0.25	67.3	80.8	86.8	56.8	0.72	≧ 0.55	67.6	84.2	80.6	72.7	0.76	≧ 0.95	70.6	84.5	57.1	90.7	0.81

APRI, aspartate aminotransferase-to-platelet ratio index; LI, liver to intervertebral disk ratio; NPV, negative predictive value; PPV, positive predictive value; Sen, sensitivity; Spe, specificity.

significant fibrosis, and extent of fibrosis and cirrhosis could be excluded with cut-offs of ≧ 1.62, ≧ 1.55, and ≧ 1.47, respectively, and the negative predictive values were 69.2%, 90%, and 96.5%, respectively. The presence of cirrhosis could be ruled out with high certainty.

Applying the low cut-off (≦ 1.38), 56 (50.9%) of the 110 patients belonging to the estimation group with significant fibrosis in the liver biopsy were correctly identified. Fifty-six of 57 patients with ≦ 1.38 showed significant fibrosis in the liver biopsy (positive predictive value 98%).

The cut-offs of ≦ 1.38 and ≦ 1.315 also showed high PPV in the extent of fibrosis or cirrhosis but were not so high. The representative cut-off points of significant and extensive fibrosis and cirrhosis were determined as 1.55, 1.51, and 1.38, respectively. Comparing the accuracy of each cut-off point, LI25 had the highest accuracy of significant fibrosis and cirrhosis, but FibroIndex was higher for the extent of fibrosis. These tendencies were also demonstrated in the validation set.

Discussion

Several studies have evaluated the use of readily available laboratory test results to predict significant fibrosis or cirrhosis in patients, such as Forn's score,[11] the FibroIndex,[12] the Lok index,[13] and APRI.[14] Because all these fibrosis markers need platelet counts and many need AST, patients whose platelet count has changed by other diseases or who have severe active hepatitis sometimes might have values largely different from actual fibrosis. Many studies have reported the evaluation of liver function or fibrosis with Gd-EOB-DTPA-enhanced MRI effects in liver damage.[20–25] RE of liver parenchyma increased significantly with time until at least 20 min in normal or moderate liver dysfunction, but Child–Pugh class C did not show any increase after the portal phase.[22] Tajima *et al.* reported that in both normal and chronic liver disease groups, liver enhancement increased gradually up to 30 min in the hepatobiliary phase, and the peak value at 30 min with normal liver function was higher than that in chronic liver dysfunction.[26]

In our data, RE gradually increased until 25 min in the hepatobiliary phase in normal liver, but in advanced liver dysfunction, RE did not increase significantly, and the ratio of RE gradually increased over time, so we decided to use data that had been calculated using several methods both at 15 and 25 min in the hepatobiliary phase to compare its accuracy and usefulness. All MRI methods at 25 min had higher AUROC and higher correlation than at 15 min (data not shown). The best correlation of MRI and the liver biopsy was with LI at 25 min, which also had the highest AUROC for discriminating significant, extensive fibrosis and liver cirrhosis in the estimation set, followed by RE, with LS being the least accurate of these four methods. The LI score at 25 min was higher than the liver function tests that were reported previously, such as Forn's score, the FibroIndex, the Lok index, and APRI. Also in the validation set, LI at 25 min had the highest score of all these predictive methods.

SI in the hepatobiliary phase may be influenced by several factors, such as decreased hepatocytes, deficiency of hepatocyte function, and indocyanine green clearance.[21,27,28] The uptake of gadoxetate disodium and its excretion are performed by the anion transporting polypeptide Oatp1 and Mrp2 mainly,[29] and the balance of these effects may decide the SI of liver parenchyma followed by a decreased signal in hepatic damage and cirrhosis.[30–32] Some previous reports have evaluated fibrosis using Gd-EOB-DTPA. Tsuda *et al.* reported the possibility of predicting fibrosis in non-alcoholic steatohepatitis (NASH) by using NASH model rats.[24,33] Watanabe *et al.* reported that Gd-EOB-DTPA correlated with the fibrosis stage, but their report had a small number of patients, included several courses of hepatic injury, and used only the LMSI ratio.[23] Many reports have used RE,[22,25] and some have used the liver-to-spleen ratio;[28] but, no reports have compared the accuracy of these methods. In chronic liver disease, especially in the advanced stage such as cirrhosis, many changes to the internal organ circulation occur, and in some cases, there may be inequality in the LMSI ratio and LSSI ratio. In this study, we tried to calculate the intensity ratio by using an internal control with intervertebral disc intensity because intervertebral discs have no enhancement after Gd-EOB-DTPA injection and compared all methods to decide the most useful method to evaluate hepatic fibrosis. LI method at 25 min had the highest AUROC in the prediction of significant or extensive fibrosis, so we recommend using LI and prefer to use the 25-min hepatobiliary data after injection. Detecting focal liver lesions 10 min after injection can be acceptable,[28] but for the purpose of fibrotic evaluation, longer sampling, such as 25 min, is recommended.

Although LI has almost the same accuracy of fibrotic evaluation as using previous reported hematologic methods (no significant differences), we can obtain high accuracy with 0.79–0.86, and these values are higher than previous serum fibrosis markers; it may be an advantage to evaluate fibrosis and scanning HCC occurrence simultaneously and especially very useful in patients that are impossible to evaluate using the platelet count because of other reasons that have changed its value. The LI method can evaluate patients who are obese or have ascites, although these patients are not suitable to evaluate by Fibroscan, which is another non-invasive method reported previously. On the other hand, there are some problems with the LI25 method: (i) In general treatment, it is sometimes slightly difficult to find the best disk position because some patients have disk disease or spinal curvature; (ii) longer time is needed to obtain these pictures because 15 min is usually enough to detect a neoplasm in the liver; and (iii) MRI is more expensive than serum examination.

It is necessary to compare our methods to other devices such as MR elastography and transient elastography (Fibroscan), and prospective studies are needed to decide the most evaluable method. At the moment, we suggest that using a combination of hematologic biomarkers may lead to more accurate diagnosis without liver biopsy. Further, using EOB-MRI has a possibility of reflecting liver function accurately rather than its fibrosis, more detailed investigation is needed of liver function and EOB-MRI.

Conclusion

EOB-MRI is a useful non-invasive method to evaluate the fibrosis of HCV-infected liver disease, and the LI at 25-min post-injection seems to be the most accurate.

References

1 Liang TJ, Rehermann B, Seeff LB, Hoofnagle JH. Pathogenesis, natural history, treatment, and prevention of hepatitis C. *Ann. Intern. Med.* 2000; **132**: 296–305.

2 Tsukuma H, Hiyama T, Tanaka S *et al.* Risk factors for hepatocellular carcinoma among patients with chronic liver disease. *N. Engl. J. Med.* 1993; **328**: 1797–801.
3 Yoshida H, Shiratori Y, Moriyama M *et al.* Interferon therapy reduces the risk for hepatocellular carcinoma: national surveillance program of cirrhotic and noncirrhotic patients with chronic hepatitis C in Japan. IHIT Study Group. Inhibition of hepatocarcinogenesis by interferon therapy. *Ann. Intern. Med.* 1999; **131**: 174–81.
4 Ikeda K, Saitoh S, Koida I *et al.* A multivariate analysis of risk factors for hepatocellular carcinogenesis: a prospective observation of 795 patients with viral and alcoholic cirrhosis. *Hepatology* 1993; **18**: 47–53.
5 Zoli M, Magalotti D, Bianchi G, Gueli C, Marchesini G, Pisi E. Efficacy of a surveillance program for early detection of hepatocellular carcinoma. *Cancer* 1996; **78**: 977–85.
6 Cottone M, Turri M, Caltagirone M *et al.* Screening for hepatocellular carcinoma in patients with Child's A cirrhosis: an 8-year prospective study by ultrasound and alphafetoprotein. *J. Hepatol.* 1994; **21**: 1029–34.
7 Oka H, Kurioka N, Kim K *et al.* Prospective study of early detection of hepatocellular carcinoma in patients with cirrhosis. *Hepatology* 1990; **12**: 680–7.
8 Perrault J, McGill DB, Ott BJ, Taylor WF. Liver biopsy: complications in 1000 inpatients and outpatients. *Gastroenterology* 1978; **74**: 103–6.
9 Wong JB, Koff RS. Watchful waiting with periodic liver biopsy versus immediate empirical therapy for histologically mild chronic hepatitis C. A cost-effectiveness analysis. *Ann. Intern. Med.* 2000; **133**: 665–75.
10 Bedossa P, Poynard T. An algorithm for the grading of activity in chronic hepatitis C. The METAVIR Cooperative Study Group. *Hepatology* 1996; **24**: 289–93.
11 Forns X, Ampurdanes S, Llovet JM *et al.* Identification of chronic hepatitis C patients without hepatic fibrosis by a simple predictive model. *Hepatology* 2002; **36**: 986–92.
12 Koda M, Matunaga Y, Kawakami M, Kishimoto Y, Suou T, Murawaki Y. FibroIndex, a practical index for predicting significant fibrosis in patients with chronic hepatitis C. *Hepatology* 2007; **45**: 297–306.
13 Lok AS, Ghany MG, Goodman ZD *et al.* Predicting cirrhosis in patients with hepatitis C based on standard laboratory tests: results of the HALT-C cohort. *Hepatology* 2005; **42**: 282–92.
14 Wai CT, Greenson JK, Fontana RJ *et al.* A simple noninvasive index can predict both significant fibrosis and cirrhosis in patients with chronic hepatitis C. *Hepatology* 2003; **38**: 518–26.
15 Castera L, Vergniol J, Foucher J *et al.* Prospective comparison of transient elastography, Fibrotest, APRI, and liver biopsy for the assessment of fibrosis in chronic hepatitis C. *Gastroenterology* 2005; **128**: 343–50.
16 Rouviere O, Yin M, Dresner MA *et al.* MR elastography of the liver: preliminary results. *Radiology* 2006; **240**: 440–8.
17 Rizzo L, Calvaruso V, Cacopardo B *et al.* Comparison of transient elastography and acoustic radiation force impulse for non-invasive staging of liver fibrosis in patients with chronic hepatitis C. *Am. J. Gastroenterol.* 2011; **106**: 2112–20.
18 Huppertz A, Balzer T, Blakeborough A *et al.* Improved detection of focal liver lesions at MR imaging: multicenter comparison of gadoxetic acid-enhanced MR images with intraoperative findings. *Radiology* 2004; **230**: 266–75.
19 Hanley JA, McNeil BJ. A method of comparing the areas under receiver operating characteristic curves derived from the same cases. *Radiology* 1983; **148**: 839–43.
20 Schuhmann-Giampieri G, Schmitt-Willich H, Press WR, Negishi C, Weinmann HJ, Speck U. Preclinical evaluation of Gd-EOB-DTPA as a contrast agent in MR imaging of the hepatobiliary system. *Radiology* 1992; **183**: 59–64.
21 Ryeom HK, Kim SH, Kim JY *et al.* Quantitative evaluation of liver function with MRI using Gd-EOB-DTPA. *Korean J. Radiol.* 2004; **5**: 231–9.
22 Tamada T, Ito K, Higaki A *et al.* Gd-EOB-DTPA-enhanced MR imaging: evaluation of hepatic enhancement effects in normal and cirrhotic livers. *Eur. J. Radiol.* 2011; **80**: e311–16.
23 Watanabe H, Kanematsu M, Goshima S *et al.* Staging hepatic fibrosis: comparison of gadoxetate disodium-enhanced and diffusion-weighted MR imaging—preliminary observations. *Radiology* 2011; **259**: 142–50.
24 Tsuda N, Okada M, Murakami T. Potential of gadolinium-ethoxybenzyl-diethylenetriamine pentaacetic acid (Gd-EOB-DTPA) for differential diagnosis of nonalcoholic steatohepatitis and fatty liver in rats using magnetic resonance imaging. *Invest. Radiol.* 2007; **42**: 242–7.
25 Kim T, Murakami T, Hasuike Y *et al.* Experimental hepatic dysfunction: evaluation by MRI with Gd-EOB-DTPA. *J. Magn. Reson. Imaging* 1997; **7**: 683–8.
26 Tajima T, Takao H, Akai H *et al.* Relationship between liver function and liver signal intensity in hepatobiliary phase of gadolinium ethoxybenzyl diethylenetriamine pentaacetic acid-enhanced magnetic resonance imaging. *J. Comput. Assist. Tomogr.* 2010; **34**: 362–6.
27 Tschirch FT, Struwe A, Petrowsky H, Kakales I, Marincek B, Weishaupt D. Contrast-enhanced MR cholangiography with Gd-EOB-DTPA in patients with liver cirrhosis: visualization of the biliary ducts in comparison with patients with normal liver parenchyma. *Eur. Radiol.* 2008; **18**: 1577–86.
28 Motosugi U, Ichikawa T, Tominaga L *et al.* Delay before the hepatocyte phase of Gd-EOB-DTPA-enhanced MR imaging: is it possible to shorten the examination time? *Eur. Radiol.* 2009; **19**: 2623–9.
29 van Montfoort JE, Stieger B, Meijer DK, Weinmann HJ, Meier PJ, Fattinger KE. Hepatic uptake of the magnetic resonance imaging contrast agent gadoxetate by the organic anion transporting polypeptide Oatp1. *J. Pharmacol. Exp. Ther.* 1999; **290**: 153–7.
30 Nakai K, Tanaka H, Hanada K *et al.* Decreased expression of cytochromes P450 1A2, 2E1, and 3A4 and drug transporters Na+-taurocholate-cotransporting polypeptide, organic cation transporter 1, and organic anion-transporting peptide-C correlates with the progression of liver fibrosis in chronic hepatitis C patients. *Drug Metab. Dispos.* 2008; **36**: 1786–93.
31 Ogasawara K, Terada T, Katsura T *et al.* Hepatitis C virus-related cirrhosis is a major determinant of the expression levels of hepatic drug transporters. *Drug Metab. Pharmacokinet.* 2010; **25**: 190–9.
32 Hinoshita E, Taguchi K, Inokuchi A *et al.* Decreased expression of an ATP-binding cassette transporter, MRP2, in human livers with hepatitis C virus infection. *J. Hepatol.* 2001; **35**: 765–73.
33 Tsuda N, Okada M, Murakami T. New proposal for the staging of nonalcoholic steatohepatitis: evaluation of liver fibrosis on Gd-EOB-DTPA-enhanced MRI. *Eur. J. Radiol.* 2010; **73**: 137–42.

J Med Ultrasonics (2013) 40:289–291
DOI 10.1007/s10396-013-0430-y

ULTRASOUND IMAGE OF THE MONTH

Bleeding in abdominal cavity revealed by contrast-enhanced ultrasonography

Shuichi Sato · Hiroshi Tobita · Tatsuya Miyake · Tsukasa Saitou · Yoshikazu Kinoshita

Received: 23 August 2012 / Accepted: 21 December 2012 / Published online: 26 April 2013

Keywords Contrast-enhanced ultrasonography · Sonazoid · Accumulation · Bleeding · Abdominal cavity

Introduction

Bleeding in the abdominal cavity can lead to hypovolemic shock and is a life-threatening condition; thus, its detection in real time is critical. Although dynamic computed tomography (CT) is useful for detecting extravasation, it may be difficult to detect slight bleeding in the abdominal cavity with that modality. We treated a patient with intra-abdominal bleeding from a ruptured hepatocellular carcinoma (HCC), which was revealed in still images obtained with contrast-enhanced ultrasonography (US) as accumulation with maximum intensity. Such accumulation with maximum intensity in still images is useful for detecting slight bleeding in the abdominal cavity.

Case presentation

A 74-year-old female with a history of HCC developed liver cirrhosis due to hepatitis C virus along with abdominal fullness and right hypochondralgia, and was referred to our hospital. Our initial examination found a distended abdomen, and blood test results revealed marked anemia (hemoglobin level 6.9 g/dL). On admission, laboratory findings showed serum albumin 3.0 g/dL, total bilirubin 1.5 mg/dL, aspartate aminotransferase 84 IU/L, alanine aminotransferase 37 IU/L, ammonia 49 μg/dL, prothrombin time 64 %, alpha-fetoprotein 87,566 ng/mL, and des-γ-carboxy prothrombin 119 mAU/mL. A digital examination did not reveal tarry or bloody stool suggesting intestinal bleeding. Plain computed tomography (CT) and B-mode US detected a 5-cm-diameter nodule on the surface of the right lobe of the liver, right portal vein tumor thrombus, and massive ascites (Figs. 1, 2). We therefore theorized that the symptoms were caused by a ruptured HCC.

For selection of initial treatment in such cases, such as blood transfusion, emergency angiography, or surgery, it is important to know whether the intra-abdominal bleeding is ongoing or stopped. The present patient had a history of shock due to contrast media injection for hepatic arterial angiography; thus, contrast-enhanced CT could not be performed to diagnose intra-abdominal bleeding, and contrast-enhanced US (CEUS) was used instead with a LOGIQ E9™ ultrasound system (GE Healthcare, Milwaukee, WI, USA). The mechanical index was adjusted to 0.2, the frame rate was 11 frames/s, and the focus point was on the deepest level of intra-abdominal fluid. The second-generation contrast agent Sonazoid™, which consists of stabilized gas microbubbles, was intravenously administered at 0.01 mg/kg body weight. Approximately 6 min after administering Sonazoid, circulating microbubbles were subtly observed, while still images did not enough to show the presence of drifting microbubbles in the echo-free space of the abdominal cavity (Fig. 3). A large number of drifting microbubbles was shown as accumulation based on maximum intensity projection (MIP) images (Fig. 4). Evaluation of hepatic function and tumor development

S. Sato (✉)
Division of Gastrointestinal Endoscopy, Shimane University Hospital, 89-1 Enya-cho, Izumo, Shimane, Japan
e-mail: bbsato@med.shimane-u.ac.jp

H. Tobita · T. Miyake · T. Saitou · Y. Kinoshita
Department of Gastroenterology and Hepatology, Shimane University Faculty of Medicine, Izumo, Japan

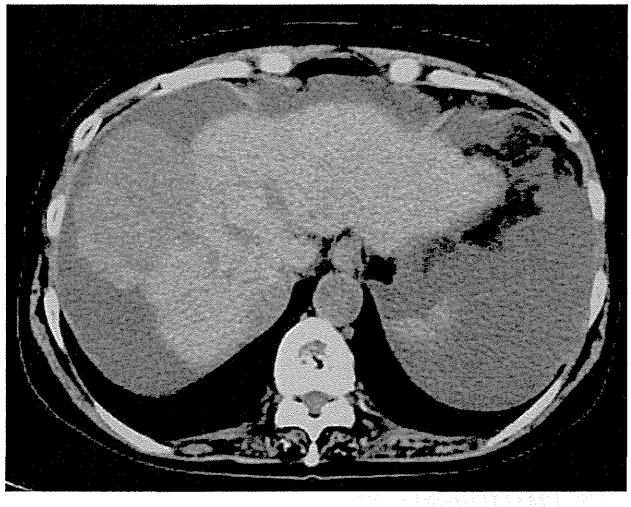

Fig. 1 Plain abdominal CT image obtained on admission showing a low-density nodule on the right lobe of the liver and massive ascites

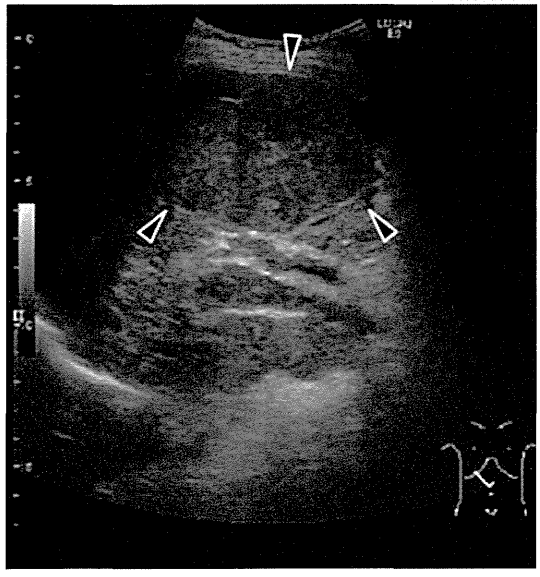

Fig. 2 B-mode US image showing a humped nodule on the right lobe of the liver (*arrowheads*), portal thrombus, and ascites

suggested that emergency interventional radiological therapy for bleeding from the ruptured HCC would not improve the patient's prognosis. Therefore, only a blood transfusion was performed as conservative treatment.

Discussion

Spontaneous rupture is a life-threatening complication of liver tumors because of potential massive blood loss into the abdominal cavity and rapidly increasing hepatic failure. Diagnosis of massive bleeding from a ruptured HCC is generally made from angiography, CT, or Doppler US findings [1]. US has excellent scale spatial resolution, and

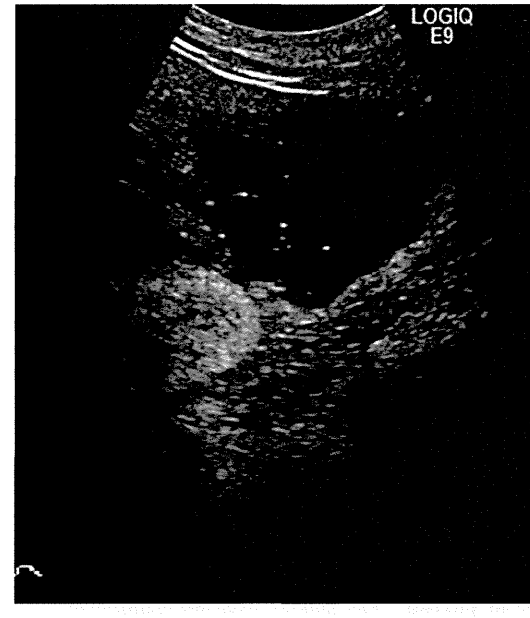

Fig. 3 Still image obtained with contrast-enhanced US with Sonazoid™. A few drifting microbubbles can be seen in the echo-free space of the abdominal cavity

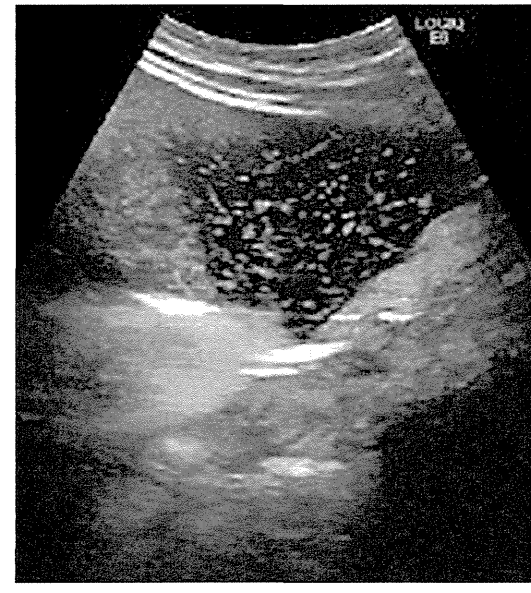

Fig. 4 Still image obtained with contrast-enhanced US with accumulation based on MIP processing. A large number of traces of drifting microbubbles in the echo-free space of the abdominal cavity can be seen

use of second-generation contrast agents such as Sonazoid has provided improved diagnostic ability for various tumors with that modality [2]. Other reports have shown the usefulness of CEUS for diagnoses of HCC differentiation [3] and an intrahepatic shunt accompanying advanced chronic liver disease along with evidence of diaphragmatic holes in patients with hepatic pleural effusion [4]. Although CEUS is also helpful for determining the bleeding point

and therapeutic strategy after diagnosis [5, 6], it is difficult to observe trace bleeding showing a possible HCC rupture in those images. In most cases, bleeding from a ruptured HCC originates from an artery. However, microbubbles were not observed until 6 min after the administration of Sonazoid in the present case, which may have been caused by pooled blood including microbubbles in the hematoma gradually released from the bleeding point in the abdominal cavity.

It is difficult to visualize subtly drifting microbubbles in echo-free space in still images. Accumulation is a state-of-the-art technique used to detect peak values, then hold and display them. It can be used with real-time imaging as well as stored cine loop images with a moving time window for processing. This technique is based on MIP processing. The present results show the utility of this technique for revealing subtly drifting microbubbles with CEUS imaging.

Conflict of interest The authors have no conflicts of interest to declare.

References

1. Ishida H, Konno K, Hamashima Y, et al. Sonographic and color Doppler findings of rupture of liver tumors. Abdom Imaging. 1998;23:587–91.
2. Moriyasu F, Itoh K. Efficacy of perflubutane microbubble-enhanced ultrasound in the characterization and detection of focal liver lesions: phase 3 multicenter clinical trial. AJR Am J Roentgenol. 2009;193:86–95.
3. Takahashi M, Maruyama H, Ishibashi H, et al. Contrast-enhanced ultrasound with perflubutane microbubble agent: evaluation of differentiation of hepatocellular carcinoma. AJR Am J Roentgenol. 2011;196:123–31.
4. Matono T, Koda M, Murawaki Y. Right diaphragmatic defect in hepatic hydrothorax exposed by contrast-enhanced ultrasonography after radiofrequency ablation. Hepatology. 2012;56:784–5.
5. Naganuma H, Funaoka M, Fujimori S, et al. Rupture of liver metastasis: report of a case with emphasis on contrast-enhanced US. J Med Ultrasonics. 2007;34:113–6.
6. Matsumoto N, Ogawa M, Nakagawara H, et al. Clinical efficacy of contrast-enhanced ultrasonography (CEUS) in the diagnosis of ruptures hepatocellular carcinoma (HCC). J Med Ultrasonics. 2007;34:101–5.

Journal of Gastroenterology and Hepatology

JGHF

doi:10.1111/jgh.12076

HEPATOLOGY

Des-gamma-carboxy prothrombin identified by P-11 and P-16 antibodies reflects prognosis for patients with hepatocellular carcinoma

Satoru Takeji,* Masashi Hirooka,* Yohei Koizumi,* Yoshio Tokumoto,* Masanori Abe,* Yoshio Ikeda,* Seijin Nadano,† Yoichi Hiasa* and Morikazu Onji*

*Department of Gastroenterology and Metabology, Ehime University Graduate School of Medicine, Toon, and †Department of Gastroenterology, National Hospital Organization Shikoku Cancer Center, Matsuyama, Ehime, Japan

Key words
AFP-L3, alpha-fetoprotein, DCP, hepatocellular carcinoma, NX-PVKA, prognosis.

Accepted for publication 24 September 2012.

Correspondence
Yoichi Hiasa, Department of Gastroenterology and Metabology, Ehime University Graduate School of Medicine, Shitsukawa, Toon, Ehime 791-0295, Japan. Email: hiasa@m.ehime-u.ac.jp

Declaration of conflict of interest: The authors declare no conflicts of interest.

Abstract

Background and Aims: Serum des-γ-carboxy prothrombin (DCP) is an established tumor marker in patients with hepatocellular carcinoma (HCC), which can be identified by using MU-3 antibody. The MU-3 antibody mainly reacts with the 9–10 glutamic acid residues of DCP (conventional DCP). Since other variants of DCP with fewer glutamic acid residues can be detected using P-11 and P-16 antibodies (code name: NX-PVKA), we examined the clinical characteristics associated with NX-PVKA, and whether NX-PVKA is a useful measure in HCC patients.

Methods: Participants comprised 197 HCC patients admitted to our hospital between 2001 and 2010. NX-PVKA, conventional DCP, alpha-fetoprotein, and L3 fraction of alpha-fetoprotein were measured prior to initiation of HCC treatment.

Results: Of the tumor markers assessed, NX-PVKA was the only significant predictor of prognosis (hazard ratio, 81.32; $P < 0.0001$). Patients with NX-PVKA level ≥ 100 mAU/mL showed significantly lower survival rates ($P < 0.0001$). NX-PVKA level was also significantly associated with platelet count, prothrombin time, C-reactive protein, sex, maximum tumor size, number of nodules, and portal venous invasion by HCC. Finally, using NX-PVKA level and other clinical parameters, we established a prognostic model to estimate patient survival time.

Conclusions: NX-PVKA offers the best marker of tumor prognosis among HCC patients, and is strongly associated with tumor factors and hepatic functional reserve. NX-PVKA could be useful for clinical evaluation of tumor severity, as well as the estimated duration of survival among patients with HCC.

Introduction

Hepatocellular carcinoma (HCC) often occurs in patients with chronic liver injury, especially those with liver cirrhosis.[1] Serum level of des-γ-prothrombin (DCP), known as protein induced by the absence of vitamin K or antagonist II (PIVKA-II), is an established tumor marker, and is significantly elevated in patients with HCC.[2,3] Clinically, DCP levels can be used as a marker of HCC among patients with chronic liver injury.[4]

DCP has several variants based on the number of glutamic acid (Glu) residues (from 0 to 10). Interestingly, the DCP variants released by HCC appear to differ from those released due to vitamin K deficiency.[5–7] Conventionally, serum levels of DCP have been identified using MU-3 monoclonal antibody (Picolumi PIVKA-II; EIDIA, Tokyo, Japan), which reportedly binds predominantly to DCP with 9–10 Glu residues, otherwise known as conventional DCP.[6] A new procedure has recently emerged for identifying the different variants of DCP using P-11 and P-16 monoclonal antibodies (Sekisui Medical, Tokyo, Japan). These new variants (code name: NX-PVKA) contain fewer Glu residues than the variants identified using the MU-3 antibody.[7] The NX-PVKA ratio (NX-PVKA-R) is calculated as the level of conventional DCP divided by NX-PVKA, and has been proposed as a useful marker for HCC patients taking warfarin.[7]

The present study measured NX-PVKA, and calculated NX-PVKA-R, as well as conventional DCP, alpha-fetoprotein (AFP), and the L3 fraction of the *Lens culinaris* agglutinin-reactive species of AFP (AFP-L3),[8,9] as established tumor markers of HCC. We then assessed associations between these values and clinical features, prognosis, liver function test parameters, and HCC tumor factors. Using these analyses, we sought to clarify the clinical characteristics associated with NX-PVKA and to assess the usefulness of this measure in patients with HCC.